RESEARCH ARTICLE   **Open Access**

Chitosan-coated sour cherry kernel shell beads: an adsorbent for removal of Cr(VI) from acidic solutions

Türkan Altun

Abstract

In this study, a composite biosorbent in the form of beads was produced from chitosan and the powder of sour cherry kernel shells. Characterization of chitosan-coated sour cherry kernel shell beads was done using elemental analysis, FT-IR spectroscopy, SEM, and EDX spectrum analysis. Adsorption capacity of chitosan-coated sour cherry kernel shell beads was tested in removal of Cr(VI) under different conditions, pH 2.0–7.0, adsorbent dosage 0.01–0.20 g, initial Cr(VI) ion concentration 10–315 mg L^{-1}, temperature 25–55 °C, and contact time 0–240 min, and compared to that of uncoated sour cherry kernel shell powder. Cr(VI) adsorption was highly dependent on the solution pH, and the maximum Cr(VI) adsorption was achieved at pH 2.03 at 25 °C in 45 min. The adsorption data was applied to Langmuir, Freundlich, Scatchard, and Dubinin-Radushkevich (D-R) adsorption isotherm models. According to the Langmuir isotherm model, the adsorption capacity of chitosan-coated sour cherry kernel shell beads was found higher than that of uncoated sour cherry kernel shell powder, 24.492 and 13.57 mg g^{-1}. The study demonstrated that chitosan-coated sour cherry kernel shell beads can be used for Cr(VI) removal from acidic aqueous solutions.

Keywords: Adsorption, Sour cherry kernel shell, Chitosan, Cr(VI), Isotherms

Introduction

Designing adsorbents from low-cost and abundant biological waste materials has attracted attention in recent years (Mohan and Pittman Jr 2006). Biomass waste from plants or animals has been widely used to produce environmentally friendly adsorbents. Biopolymers are considered to be an abundant, renewable, biodegradable, and low-cost source of material for the production of adsorbents. These properties make adsorbents with biological origins much more attractive than synthetic adsorbents (Wang and Chen 2009).

Chitin is an excellent structural biopolymer. Chitin is found in many organisms including insects, mushrooms, and arthropods (Kaya et al. 2013). Chitin is easily obtained from, for example, waste of crabs in food processing industry using simple acidic, alkaline, and depigmentation treatments. Then, it is converted into chitosan, a more versatile derivative, through deacetylation procedure

under hot alkaline conditions. In deacetylation treatment, free pendant amino groups are formed on the polymeric backbone of chitosan (Ali 2010). These free amino groups make chitosan soluble in acidic solutions and suitable for further modifications. Compared to chitin, chitosan has wider applications due to its gel-forming nature, solubility, and affinity for metal ions (Miretzky and Cirelli 2009, Wu et al. 2010).

Amino and hydroxyl groups are responsible for the affinity of chitosan for metal ions. Protonation of $-NH_2$ and $-OH$ groups enhances the electrostatic interaction of chitosan with negatively charged species (Gupta and Balomajumder 2015). Chitosan in gel form is soluble in acidic environments. It should be stabilized when used in acidic aqueous solutions. Free amino groups of chitosan also enable cross-linking of the polymeric backbone of chitosan. Free amino groups react readily with carbonyl groups of aldehydes. Glutaraldehyde is widely used as a cross-linking agent for chitosan. In the cross-linking procedure, carbonyl groups of glutaraldehyde form Schiff bases with amino functional groups of chitosan.

Correspondence: turkanaltun@yahoo.com
Department of Chemical Engineering, Faculty of Engineering, Selcuk University, Konya, Turkey

Once cross-linked, chitosan is no longer soluble and can be used in acidic or alkaline aqueous solutions. Through cross-linking procedure, chitosan gel can be used to immobilize micro-sized particles (Sargin and Arslan 2015).

Hexavalent chromium, Cr(VI), is a highly toxic pollutant occurring in the effluents of a number of industries including mining, electroplating, tanning, and fertilizer (Nyangababo et al. 2005). Since it is capable of bio-accumulating in the body especially in the liver, stomach, and kidneys, its removal from the aquatic environment is of utmost importance (Moon et al. 2009, Elwakeel et al. 2018). Cr(VI) is found in aqueous solutions as anions in forms of CrO_4^{2-}, $Cr_2O_7^{2-}$, and $HCrO_4^-$ (Chen et al. 2010), and these anions are cited as mutagenic and carcinogenic at concentrations higher than 0.05 mg L^{-1} (Gupta and Balomajumder 2015).

Fruit stones are considered as a major source of biomass (Lussier et al. 1994). Stones of many fruits including cherry, date, olive, apricot, and peach are a major source of biomass in the food industry. Fruit stones are widely used in the production of activated carbon (Lussier et al. 1994; Fadhil and Deyab 2008) and adsorbents for the removal of heavy metal pollutants (Strelko Jr et al. 2002, Ahmed and Theydan 2012).

Sour cherry cultivation is very common in Konya, Turkey. Therefore, there are many juice factories using sour cherries for the production of fruit juice. In the literature, there is no report on the use of sour cherry kernel shells for removal of heavy metals. This low-cost waste from the beverage industry can be used as an environmentally friendly adsorbent for heavy metal removal. Using a simple modification, this waste biomass can be used with chitosan to produce microcapsules (composite beads). Immobilization of sour cherry stone
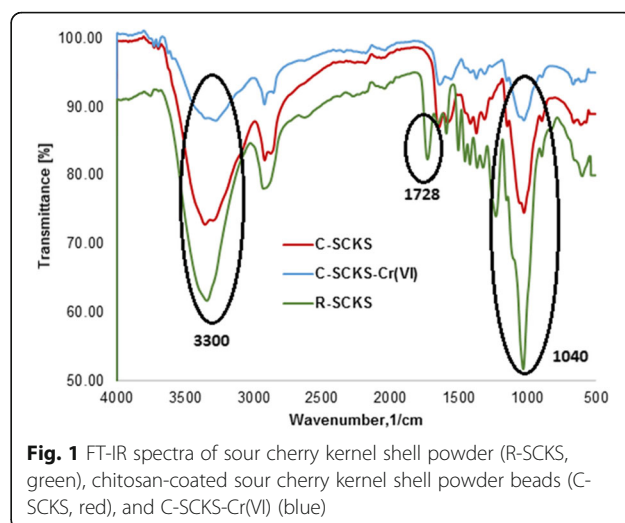

Fig. 1 FT-IR spectra of sour cherry kernel shell powder (R-SCKS, green), chitosan-coated sour cherry kernel shell powder beads (C-SCKS, red), and C-SCKS-Cr(VI) (blue)

powder in chitosan beads can enhance its adsorption capacity and can also make the use of sour cherry stones in sorption studies possible.

In this study, a new adsorbent was prepared from the powder of sour cherry stones and chitosan. Chitosan was used to immobilize the powder of sour cherry kernel shell and to enhance the affinity of shell powder entrapped in the chitosan polymeric matrice for Cr(VI) ions. Adsorptive behavior of the chitosan-coated sour cherry stone shell was tested in the removal of Cr(VI).

Materials and methods
Materials
Chemicals used in this study were of analytical grade. Medium molecular weight chitosan in powder form, $K_2Cr_2O_7$, and NaOH were purchased from Sigma-Aldrich. Glutaraldehyde, 25% aqueous solution, acetic acid, and HCl were obtained from Merck. Methanol and ethanol were from AnalaR Normapur. Stock solution of Cr(VI) was prepared from $K_2Cr_2O_7$. Aqueous acetic acid solution was used to dissolve chitosan powder. Alkaline methanol solution was used as a coagulation media. Glutaraldehyde in methanol was used as a cross-linking agent. Sour cherries were obtained from a local market in Konya, Turkey.

Preparation of chitosan-coated sour cherry kernel shells
After removing the flesh of sour cherry fruits, sour cherry stones were washed and the kernels were removed. Then, hard shells were dried at 60 °C in an oven for 24 h. Dried shells were ground and sieved with a 125-μ size sieve. Shell powder was rested in 0.1 M HCl solution, washed extensively with distilled water to neutrality, and then dried at room temperature. This kernel shell powder was called as raw sour cherry kernel shell (R-SCKS).
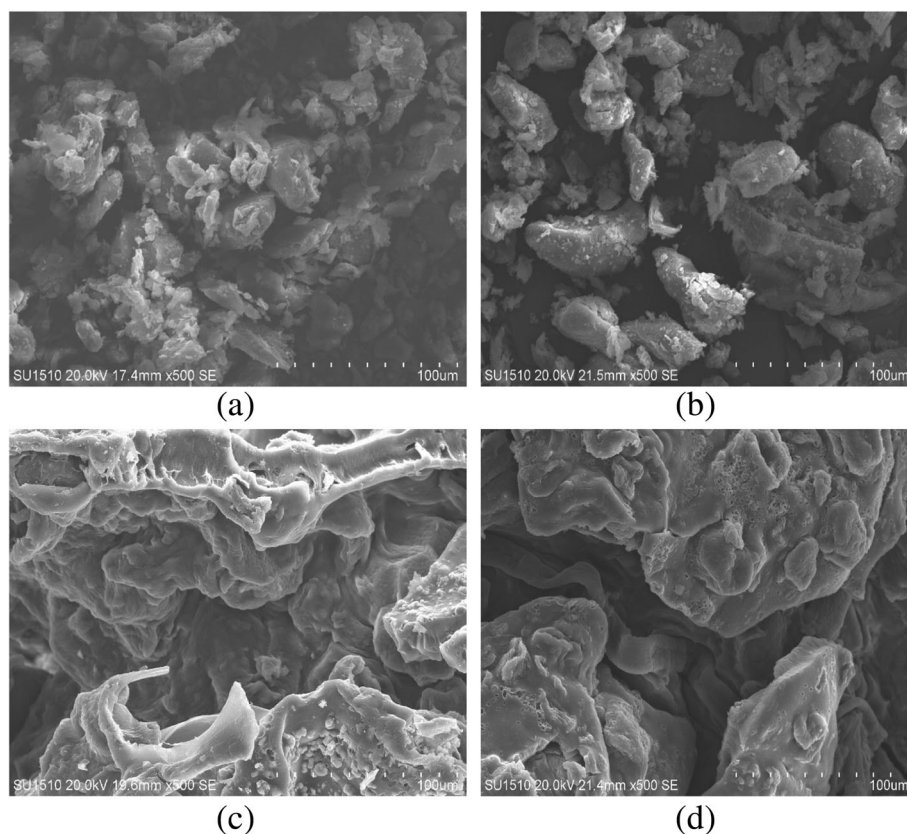
Table 1 The results of structural and elemental analyses of sour cherry kernel shell powder (R-SCKS) and chitosan-coated sour cherry kernel shell powder beads (C-SCKS)

Adsorbents	R-SCKS	C-SCKS
Structural analysis (on basis of dry weight %)		
Ash	1.490	–
Extractive	6.98	–
Hemicellulose	36.65	–
Lignin	37.2	–
Cellulose	17.68	–
Elemental analysis (%)		
C^x	47.95	42.88
H^x	6.29	5.95
O^x	44.65	48.22
N^x	1.11	2.95

^{x}Dry and no ash (at 900 °C)

Fig. 2 SEM micrograph of **a** sour cherry kernel shell powder (R-SCKS), **b** R-SCKS-(VI), **c** chitosan-coated sour cherry kernel shell powder beads (C-SCKS), and **d** C-SCKS-Cr(VI)

Chitosan solution was prepared by dissolving 1.0 g of chitosan in 50 mL of acetic acid solution (2% by volume). Following the addition of 0.5 g of shell powder, the chitosan solution was stirred for 2 h to achieve a complete dispersion of shell particles in the solution. Chitosan-shell mixture was transferred into a burette and dropped into a coagulation solution (a solution of 30 g of NaOH, 100 mL of distilled water, and 150 mL of methanol) (Sargın and Arslan 2015). To ensure a complete coagulation, chitosan-shell powder beads (C-SCKS) were rested in the coagulation solution for 24 h. C-SCKS beads were then collected and washed with distilled water to neutrality. Wet C-SCKS beads were treated with glutaraldehyde solution (0.3 mL of glutaraldehyde in 30 mL of methanol) to cross-link chitosan chains (otherwise, uncross-linked polymer would be soluble in acidic solutions) and to provide additional adsorption sites on the beads. In the cross-linking treatment, C-SCKS beads were heated at 70 °C under reflux for 6 h. Finally, cross-linked C-SCKS beads were recovered by filtration and washed with ethanol and distilled water to rid of any unreacted glutaraldehyde molecules. Cross-linked C-SCKS beads were dried at room temperature prior to use.

The adsorbents C-SCKS beads and R-SCKS were characterized through structural, elemental, FT-IR, and SEM-EDX analyses. Elemental analysis was done on a Perkin Elmer Elemental Analyser Model 240 (TUBITAK-Ankara Test and Analysis Laboratory). Structural analysis was performed according to the method reported elsewhere (Li et al. 2004).

Batch Cr(VI) adsorption experiments

A stock solution of Cr(VI) was prepared by dissolving $K_2Cr_2O_7$ in deionized water. Cr(VI) solutions were prepared by dilution of this stock solution. For pH adjustments, 0.1 M HCl and 0.1 M NaOH solution were used. pH measurements were done on an Orion 900 S2 pH meter.

In adsorption studies, two types of adsorbents were used: composite chitosan-coated kernel shells (C-SCKS beads) and uncoated kernel shell powder (R-SCKS). Their adsorptive behavior was tested in the removal of Cr(VI) ions from aqueous solutions. In Cr(VI) adsorption studies, five parameters were studied: pH (2.0–7.0), adsorbent dosage (0.01–0.20 g), initial metal ion concentration (10–315 mg/L), temperature (25–55 °C) and contact time (0–240 min). pH of the solution was varied in

Fig. 3 SEM-EDX spectra of **a** R-SCKS-Cr(VI) and **b** C-SCKS-Cr(VI)
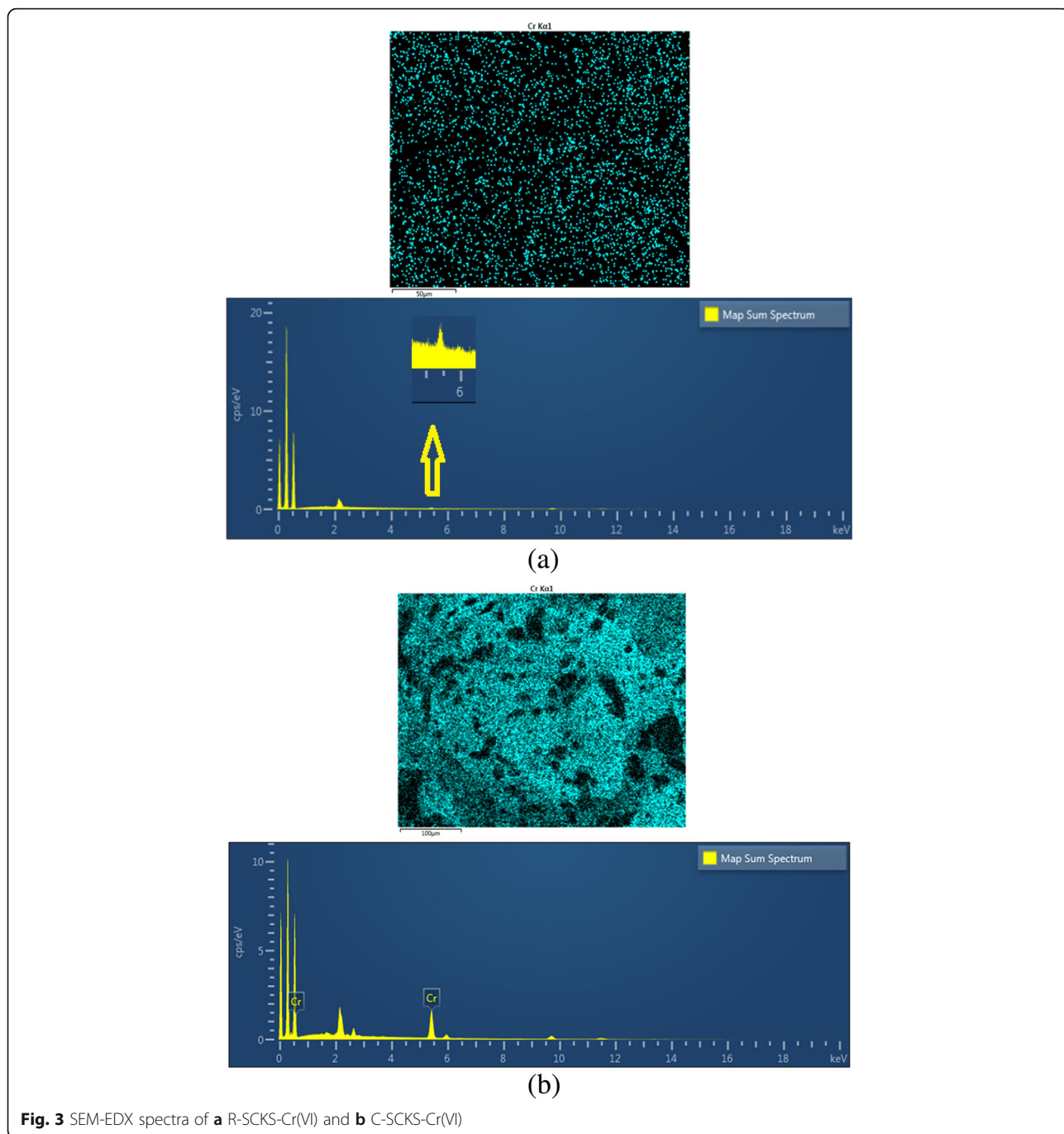
the range of pH 2.0–7.0. Test studies showed that Cr(VI) adsorption was highly dependent on the solution pH.
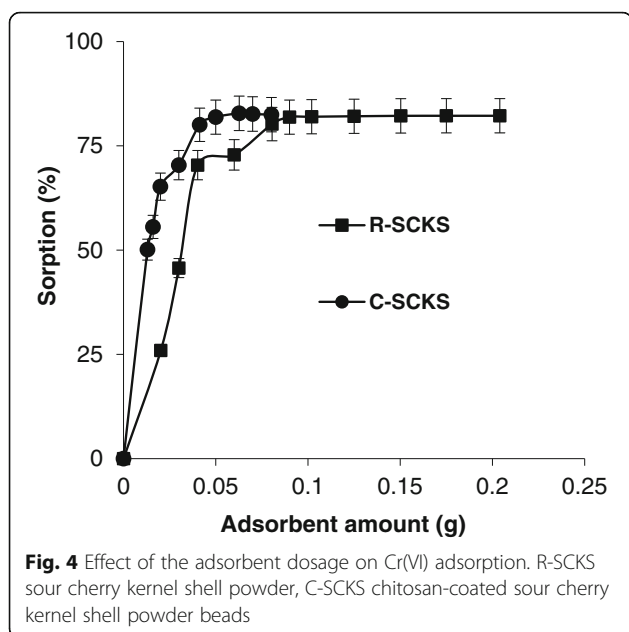
In adsorption studies, kernel shell powder (R-SCKS, 0.1 g) and chitosan-coated kernel shell powder (C-SCKS, 0.05 g) were added into Cr(VI) solutions (10 mL, 55 mg/ L at pH 2.0). The adsorbent-metal systems were stirred on magnetic stirrers at 200 rpm for 2 h. Then, the used adsorbents were filtered with a filter paper and Cr(VI) ion concentration of the filtrate was determined on a UV-visible spectrophotometer (Shimadzu UV-1700).

Absorbance measurements were done in the range of 200–600 nm and the maximum absorbance for Cr(VI) ions was recorded at 540 nm.

The equilibrium adsorption capacity of Cr(VI) (q_e) (mmol g^{-1}) was calculated using the following equation:

$$q_e = \frac{(C_i - C_e)V}{W} \tag{1}$$

where C_i and C_e are the initial and equilibrium

Fig. 4 Effect of the adsorbent dosage on Cr(VI) adsorption. R-SCKS sour cherry kernel shell powder, C-SCKS chitosan-coated sour cherry kernel shell powder beads
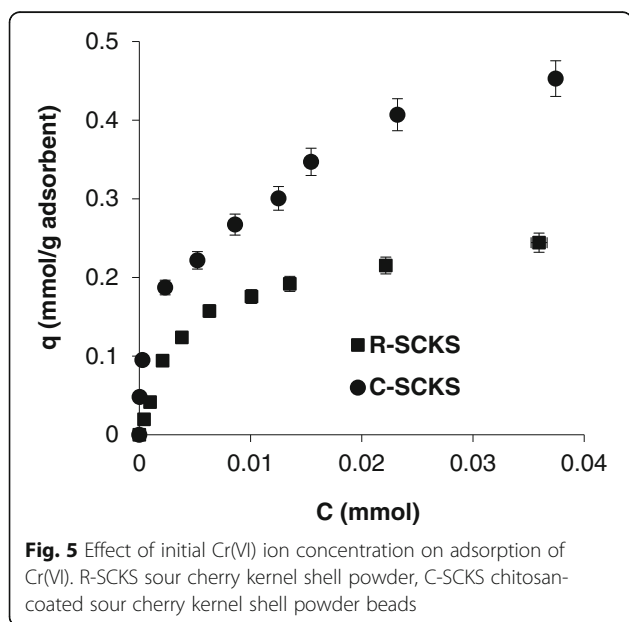
concentrations of Cr(VI) in mmol L^{-1}, V is the volume of aqueous solution of Cr(VI) (L), and W is the mass of adsorbents R-SCKS or C-SCKS (g).

Results and discussion
Characterization of the adsorbents
The chemical composition of the adsorbents (chitosan-coated kernel shell powder (C-SCKS) beads and un-coated kernel shell powder (R-SCKS)) was investigated through structural and elemental analyses, FT-IR spectroscopy, SEM micrograph, and EDX spectra. The results of the structural and elemental analyses are

Fig. 5 Effect of initial Cr(VI) ion concentration on adsorption of Cr(VI). R-SCKS sour cherry kernel shell powder, C-SCKS chitosan-coated sour cherry kernel shell powder beads

presented in Table 1. FT-IR spectra of R-SCKS, C-SCKS, and C-SCKS-Cr(VI) are presented in Fig. 1.

As listed in Table 1, C-SCKS adsorbent had higher oxygen and nitrogen content when compared to R-SCKS. This can be attributed to oxygen- and nitrogen-containing functional moieties of chitosan: OH, $-NH_2$, $-CO$.

As seen in Fig. 1, major vibration bands on chitosan and sour cherry kernel shell were present after mixing both components together. Following the interaction with Cr(VI) ions, the broader bands such as N–H and O–H groups of chitosan or the kernel shell appeared at around $3300\,cm^{-1}$ and $1040\,cm^{-1}$ (skeletal vibration of C–O of chitosan or cellulosic structures of the kernel shell) was observed. The band appearing at $1728\,cm^{-1}$ can be attributed to the carbonyl groups of kernel shell. This band was also observed in the spectrum of C-SCKS beads, but it did not appear in the spectrum of Cr(VI)-adsorbed C-SCKS beads. Following the adsorption of Cr(VI), the bands in the spectrum of C-SCKS were shifted to higher wavenumbers. Also, the presence of Cr(VI) ions led to a decrease in the absorption bands, suggesting adsorption of Cr(VI) by the adsorbent.

SEM analysis was used for the determination of surface morphology of R-SCKS, C-SCKS, R-SCKS-Cr(VI), and C-SCKS-Cr(VI). When looking at the SEM micrographs from Fig. 2, it was seen that after the adsorption of Cr(VI) for both adsorbents, the number of the particles on the surface increased and the gaps on the surface were filled. Compared to Fig. 2a and c, the rough structure of Fig. 2b and d was caused by the deposition of Cr(VI) during adsorption (Sari et al. 2017).

Besides, after the adsorption of Cr(VI) in both adsorbents, SEM-EDX analysis spectra (Fig. 3) were analyzed. In these spectra, the presence of the peaks of Cr(VI) was observed and in Fig. 3a and b, and Cr(VI) appears to be homogeneously distributed on the surface of the adsorbents. These results showed that Cr(VI) was kept on the surface for both adsorbents (Jiang et al. 2018). The uptake of Cr(VI) ions by the adsorbent was revealed by the EDX spectra (Fig. 3a, b). The affinity of chitosan for Cr(VI) ions can be seen from EDX spectra of Cr(VI)-loaded C-SCKS.

Cr(VI) adsorption studies
Adsorbent dosage
Effect of adsorbent dosage on Cr(VI) adsorption was studied under the specified conditions: 25 °C, 61 mg/L of Cr(VI), pH 2.03, and contact time 120 min.

Adsorbent dosage for R-SCKS was studied between 0.02 and 0.204 g, while for C-SCKS was between 0.013 and 0.0802 g. The results were presented in Fig. 4. As seen from the figure, the critical adsorption dosage for C-SCKS was observed at around 0.05 g where the

Table 2 The parameters of Freundlich, Langmuir, Scatchard, and D-R isotherms for adsorption of Cr(VI) by sour cherry kernel shell powder (R-SCKS) and chitosan-coated sour cherry kernel shell powder beads (C-SCKS)

Cr^{6+} adsorbents	Freundlich isotherm			Langmuir isotherm			Scatchard isotherm				D–R isotherm		
	k	n	R^2	K_b	A_s	R^2	K_s	Q_s	R^2	X_m	K	E	R^2
R-SCKS	1.457	2.12	0.959	260.4	0.261	0.993	394.98	0.232	0.932	0.416	0.0066	8.704	0.993
C-SCKS	1.265	3.153	0.996	255.8	0.471	0.960	117.68	0.545	0.915	2.049	0.0037	11.625	0.969

maximum Cr(VI) adsorption was recorded. The optimum amount was found to be 0.10 for R-SCKS. This amount was twice as much as that of C-SCKS, indicating the efficiency of C-SCKS.

Cr(VI) concentration

The effect of concentration on Cr(VI) adsorption was tested at various concentrations of Cr(VI) ions: 12.7, 26.6, 60.8, 85.2, 115.2, 144.6, 170.5, 228.6, 314.0 ppm (25 °C, pH 2.03, adsorbent dosage 0.05 g (C-SCKS) and 0.1 g (R-CSKS), and contact time 120 min) (Fig. 5). Cr(VI) adsorption equilibrium data were evaluated by using Freundlich, Langmuir isotherm, the Scatchard plot analysis, and the Dubinin-Radushkevich (D-R) model (Edebali and Pehlivan 2016; Parlayici and Pehlivan 2017). The Freundlich isotherm constants are obtained by plotting log q_e against log C_e using the linearized form of the model:

$$\log q_e = \log K_F + (1/n) \, \log C_e \tag{2}$$

where q_e is the mass of metal ion sorbed by the sorbent (in mg g^{-1}), C_e is the equilibrium metal ion concentration (in mmol L^{-1}), and k (mmol g^{-1}) and n are the Freundlich constants denoting the adsorption capacity and the intensity.

The Langmuir model is expressed in linear form as the following: the adsorption capacity A_s (in mmol g^{-1}) and the energy of adsorption K_b (in L mmol^{-1}) are calculated from the slope and intercept of the plot of C_e/q_e vs. C_e:

$$C_e/q_e = C_e/A_s + 1/(A_s K_b) \tag{3}$$

where q_e is the mass of metal ion adsorbed onto the sorbent (in mmol g^{-1}) and C_e is the equilibrium concentration of metal ion (in mmol L^{-1}).

The Scatchard plot analysis is expressed as follows:

$$q_e/C_e = K_s \, (Q_s - q_e) \tag{4}$$

where C_e is the equilibrium concentration of Cr(VI) in mmol L^{-1}, q_e is the equilibrium metal ion adsorption capacity in mmol L^{-1}, and K_s (in L mmol^{-1}) and Q_s (in mmol g^{-1}) are the Scatchard isotherm constants.

The D-R model:

$$\ln X = \ln X_m - KE^2 \tag{5}$$

where E (Polanyi potential) is [RT ln (1 + (1/Ce))], X and X_m in mmol g^{-1}, and K in mol^2 kJ^{-2}.
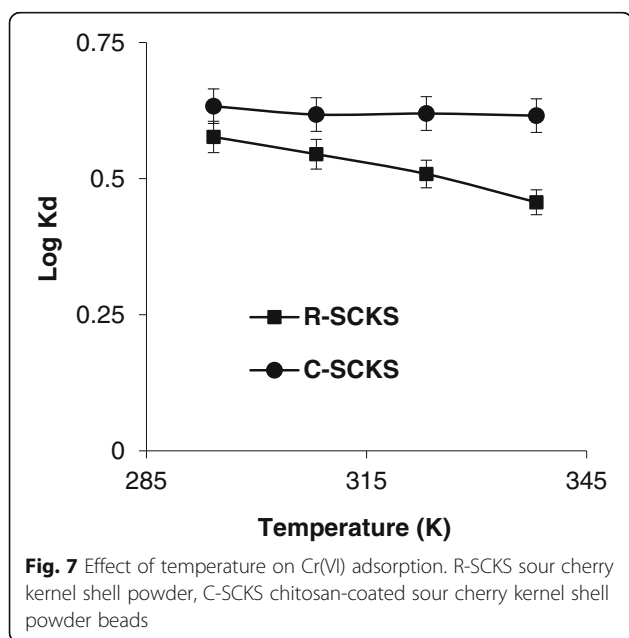
The parameters and correlation coefficients obtained from the plots of Freundlich, Langmuir, Scatchard, and D-R are listed in Table 2.

Table 3 Adsorption capacities of some adsorbents for Cr(VI) removal

Adsorbent	Maximum adsorption capacity (mg/g)	Literature
Rice husk carbon	8.80	(Ali 2010)
Natural bentonite	5.50	(Ali 2010)
Citric acid modified walnut shell	30.99	(Altun and Pehlivan 2012)
Modifying Turkish perlite with -MnO$_2$	7.60	(Edebali 2015)
Modifying Turkish perlite with -Fe$_2$O$_3$	8.64	(Edebali 2015)
Fe$_3$O$_4$/Alginate-Ce^{3+} magnetic composite beads	14.29	(Gopalakannan and Viswanathan 2015)
Citric acid modification of peach kernel shell	25.71	(Parlayıcı 2018)
γ-Fe$_2$O$_3$ nanocrystals	12.50	(Tahar et al. 2018)
Magnetic magnetite (Fe$_3$O$_4$) nanoparticles	34.87	(Rajput et al. 2016)
Coconut charcoal	5.26	(Wu et al. 2013)
Bamboo charcoal grafted by Cu^{2+}-N-aminopropylsilane complexes	17.94	(Wu et al. 2017)
Chitosan-coated sour cherry kernel shell beads (C-SCKS)	24.49	Present work
Sour cherry kernel shell powder (R-SCKS)	13.57	Present work

Fig. 6 Effect of pH on Cr(VI) adsorption. R-SCKS sour cherry kernel shell powder, C-SCKS chitosan-coated sour cherry kernel shell powder beads
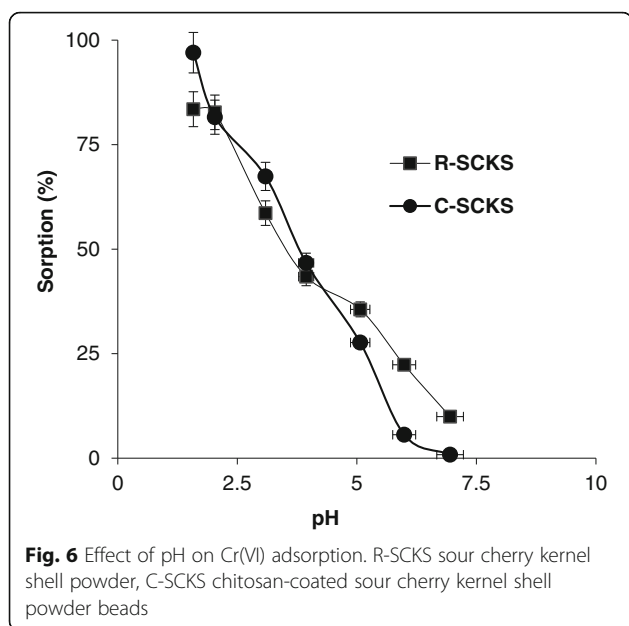
In the Scatchard plot analysis of Cr(VI) adsorption onto the adsorbents, the plot of q_e/C_e against q_e gave the straight line with high regression coefficients (R-SCKS, R^2 0.932 and C-SCKS, R^2 0.915), indicating that the adsorbent surfaces were homogenous and the metal ion sorption occurred through one type binding site (Akar et al. 2008). Also, based on the model assumptions, relatively high regression coefficients (R^2 0.993) from the Langmuir model analysis demonstrated the homogeneity of the sorption sites on the adsorbent R-SCKS (Karimi et al. 2015, Pandey and Ramontja 2016).

Fig. 7 Effect of temperature on Cr(VI) adsorption. R-SCKS sour cherry kernel shell powder, C-SCKS chitosan-coated sour cherry kernel shell powder beads

Sorption system of Cr(VI) with C-SCKS was found to best fit to the Freundlich isotherm model with R^2 0.996, indicating that the heterogeneity of the surface and the multilayer metal ion adsorption.

In the analysis of experimental data through D-R model, the value of E was found to be higher than $8\,kJ\,mol^{-1}$ and lower than $16\,kJ\,mol^{-1}$, demonstrating that the adsorption process by C-SCKS is supposed to proceed through ion exchange rather than physical interaction. In the case of R-SCKS, the value of E was about $8\,kJ\,mol^{-1}$ and the adsorption by R-SCKS can be considered to be a physical mechanism (Tuzen and Sarı 2010).

Cr(VI) adsorption capacity of the R-SCKS and C-SCKS adsorbents and the literature reports were listed in Table 3. As seen from the table, R-SCKS and C-SCKS adsorbents had moderate Cr(VI) adsorption capacity. Especially, C-SCKS adsorbent can be used in Cr(VI) removal operations.

Effect of pH
Adsorption experiments were repeated for metal ion solutions with varying pH values (1.58, 2.03, 3.09, 3.94, 5.07, 5.99, and 6.95) (Cr(VI) ion concentration 61 mg g^{-1}, temperature 25 °C, the mass of adsorbents 0.1 g (R-SCKS) and 0.05 g (C-SCKS), contact time 120 min). The effect of solution pH on the adsorption is depicted in Fig. 6. As presented in the figure, changes in Cr(VI) solution pH had a drastic effect on the adsorption process. Cr(VI) adsorption dropped sharply as the solution pH increased. A similar behavior was observed for R-SCKS and C-SCKS. The higher adsorption of Cr(VI) occurred under acidic conditions and at the lowest pH value yielded the maximum adsorption for both adsorbents. Cr(VI) occurs in aqueous solutions as anions in forms of CrO_4^{-2}, $Cr_2O_7^{-2}$, and $HCrO_4^{-}$ (Chen et al. 2010). It appears that the protonation of negatively charged functional moieties on the adsorbents enhanced Cr(VI) ions adsorption. On the other hand, lower adsorption at higher pH values can be ascribed to the electrostatic repulsion between Cr(VI) species and deprotonation of functional groups on the adsorbents and to the competition of Cr(VI) anions with OH^{-}. More efficient Cr(VI) adsorption by the adsorbent C-SCKS could have resulted from the protonated amino groups ($-NH_3^{+}$) groups of chitosan.

Thermodynamic analysis
To study the effect of temperature on Cr(VI) adsorption, equilibrium experiments were conducted at four different temperatures (298.15, 308.15, 323.15, and 338.15 K) (Cr(VI) ion concentration 61 mg L^{-1}, pH 2.03, contact time 120 min, and adsorbent dosage 0.05 g for C-SCKS and 0.1 g for R-SCKS) (Fig. 7). Thermodynamics

Table 4 Thermodynamic parameters for the adsorption of Cr(VI) by sour cherry kernel shell powder (R-SCKS) and chitosan-coated sour cherry kernel shell powder beads (C-SCKS)

Cr(VI) adsorbents	$\Delta H°$ (J.mol^{-1})	$\Delta S°$ (J.K^{-1} mol^{-1})	$\Delta G°$(J.mol^{-1})			
			$T = 298.15$ K	$T = 308.15$ K	$T = 323.15$ K	$T = 338.15$ K
R-SCKS	0.01	14.00	− 4104.98	− 4315.02	− 4525.07	− 4735.11
C-SCKS	0.06	27.81	− 8153.21	− 8570.40	− 8987.59	− 9404.78

evaluation showed the feasibility of Cr(VI) sorption by the adsorbents at studied temperatures.

The logarithm of the distribution coefficient values (K_D) were plotted against temperature (1/T). By using the slope ($\Delta H°/2.303R$) and the intercept ($\Delta H°/2.303R$) of the plot and the van't Hoff equation, changes in Gibbs free energy ($\Delta G°$), enthalpy ($\Delta H°$), and entropy ($\Delta S°$) were calculated (Table 4).

$$\log K_D = \left(\Delta S°/2.303R \right) - \left(\Delta H°/2.303RT \right) \qquad (6)$$

$$\Delta G° = \Delta H° - T\Delta S° \qquad (7)$$

where R is universal gas constant (8.314 J mol^{-1} K^{-1}) and T is the temperature (K).

The sorption system of Cr(VI) by C-SCKS and R-SCKS showed a similar characteristic. The sorption of Cr(VI) by the adsorbents was exothermic in nature (negative $\Delta H°$) and positive $\Delta S°$ exhibited that randomness in the systems increased. This increased randomness in the sorption system can be attributed to the transferring of the species with more energy from the sorption sites to the bulk phase following the adsorption of Cr(VI) ions onto the surfaces (Liu et al. 2011). $\Delta G°$ values were found to be negative for both adsorbent systems, showing that Cr(VI) sorption was spontaneous.
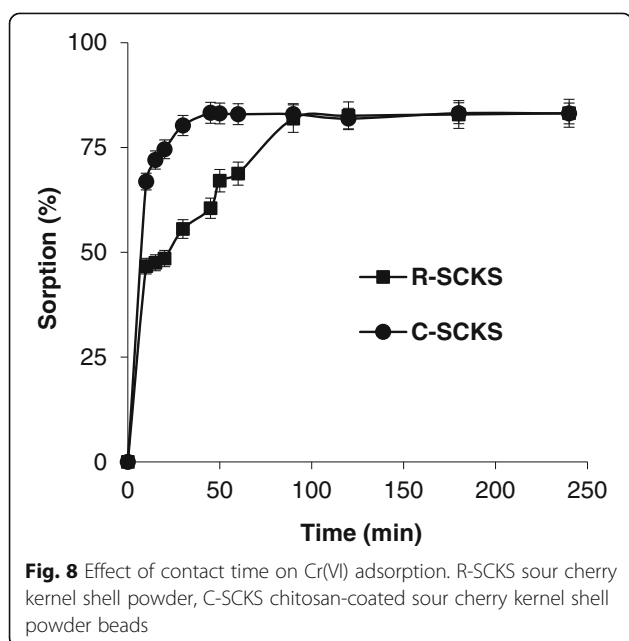

Fig. 8 Effect of contact time on Cr(VI) adsorption. R-SCKS sour cherry kernel shell powder, C-SCKS chitosan-coated sour cherry kernel shell powder beads

The negative $\Delta G°$ for both sorption systems revealed that sorption of Cr(VI) by the adsorbents was favorable at the specified conditions.

Contact time
Contact time studies were done for 10, 15, 20, 30, 45, 50, 60, 90, 120, 180, and 240 min (temperature 25 °C, Cr(VI) ion concentration 61 mg L^{-1}, pH 2.03, and adsorbent dosage 0.05 g for C-SCKS and 0.1 g for R-SCKS) (Fig. 8).

In the Cr(VI)–C-SCKS system, the sorption was relatively faster and an equilibrium was reached in the first 50 min whereas an equilibrium was observed after 100 min for Cr(VI)-R-SCKS system. Longer contact time did not contribute much to the sorption capacity of both adsorbents. As a result, the optimum contact time was recorded as 45 min for the adsorbents C-SCKS and 90 min for R-SCKS.

Repeatability of the method
Cr(VI) sorption studies by C-SCKS and R-SCKS were repeated three times at the optimum conditions to test batch-to-batch variations (C-SCKS 25 °C, 61 mg/L Cr(VI) solution, pH 2.03, 0.05 g adsorbent amount, 45 min and R-SCKS 25 °C, 61 mg/L Cr(VI) solution, pH 2.03, 0.1 g adsorbent amount, 90 min). Adsorption percentage of C-SCKS was found as 85.63; 85.57, and 85.70% and adsorption percentage of R-SCKS were 82.50; 82.37, and 82.60%. The repeatability revealed that the method used in the study was reliable and batch-to-batch variations were negligible.

Desorption studies
Regeneration of the used adsorbents is an important part of the sorption studies. Using a regeneration procedure makes it possible to recover the adsorbed Cr(VI) ions from the solution and re-use of the adsorbent over. Regeneration also makes the adsorption process convenient and cheap. In the study, the regeneration experiments were done as follows: Cr(VI)-loaded R-SCKS or C-SCKS adsorbents were dried in an oven at 65 °C and then put into 1.0 M NaOH solution and shaken for 24 h. This procedure was repeated four times using the same adsorbent (Fig. 9). The desorption capacity of C-SCKS adsorbent was found to be higher (97.63%). The results
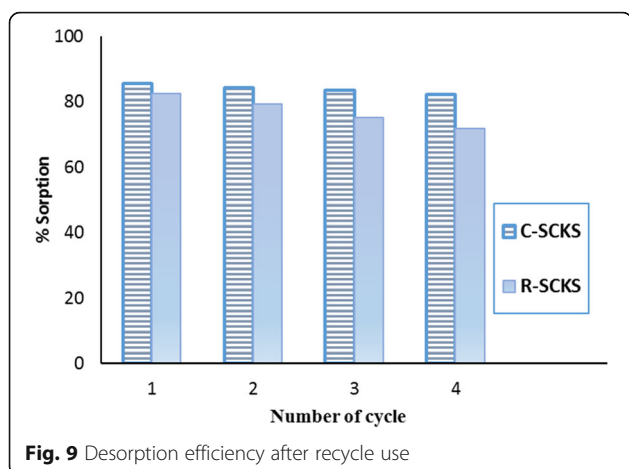
Fig. 9 Desorption efficiency after recycle use

showed that the adsorbent C-SCKS can be used in operations requiring reusability of the adsorbent.

Conclusions

This study reports an easy way for the production of biosorbent from the most abundant structural biopolymers in nature, cellulosic materials from plants and chitin from certain animals. The findings demonstrated that chitosan, a deacetylated derivative of chitin, was an excellent biopolymer for coating of powdered cellulosic materials from plants. Chitosan itself has an affinity for metal ions especially due to its hydroxyls and amino groups. It was observed that chitosan served as an immobilizing matrice for the powder of sour cherry kernel shells and enhanced their Cr(VI) adsorption capacity to some extent. Composite chitosan-coated kernel shell beads can be used as an effective biosorbent in the removal of Cr(VI) ions from acidic wastewater.

Abbreviations
C-SCKS: Chitosan-coated sour cherry kernel shell powder beads; D-R: Dubinin-Radushkevich; R-SCKS: Raw sour cherry kernel shell

Availability of data and materials
All data generated or analysed during this study are included in this published article.

Author's contributions
TA is the only author of the manuscript. All studies, adsorption studies, characterization analysis, etc. mentioned in the article were performed by the author. The author read and approved the final manuscript.

Competing interests
The author declares that she has no competing interests.

Publisher's Note
Springer Nature remains neutral with regard to jurisdictional claims in published maps and institutional affiliations.

References
Ahmed MJ, Theydan SK. Equilibrium isotherms, kinetics and thermodynamics studies of phenolic compounds adsorption on palm-tree fruit stones. Ecotoxicol Environ Saf. 2012;84:39–45.

Akar T, Ozcan AS, Tunali S, Ozcan A. Biosorption of a textile dye (Acid Blue 40) by cone biomass of Thuja orientalis: estimation of equilibrium, thermodynamic and kinetic parameters. Bioresour Technol. 2008;99(8):3057–65.

Ali I. The quest for active carbon adsorbent substitutes: inexpensive adsorbents for toxic metal ions removal from wastewater. Sep Purif Rev. 2010;39(3–4):95–171.

Altun T, Pehlivan E. Removal of Cr (VI) from aqueous solutions by modified walnut shells. Food Chem. 2012;132(2):693–700.

Chen S, Yue Q, Gao B, Xu X. Equilibrium and kinetic adsorption study of the adsorptive removal of Cr (VI) using modified wheat residue. J Colloid Interface Sci. 2010;349(1):256–64.

Edebali S. Alternative composite nanosorbents based on Turkish perlite for the removal of Cr (VI) from aqueous solution. J Nanomater. 2015;697026.

Edebali S, Pehlivan E. Evaluation of chelate and cation exchange resins to remove copper ions. Powder Technol. 2016;301:520–5.

Elwakeel KZ, Al-Bogami AS, Elgarahy AM. Efficient retention of chromate from industrial wastewater onto a green magnetic polymer based on shrimp peels. J Polym Environ. 2018;26(5):2018–29.

Fadhil AB, Deyab MM. Conversion of some fruit stones and shells into activated carbons. Arab J Sci Eng. 2008;33(2A):175–84.

Gopalakannan V, Viswanathan N. Synthesis of magnetic alginate hybrid beads for efficient chromium (VI) removal. Int J Biol Macromol. 2015;72:862–7.

Gupta A, Balomajumder C. Simultaneous adsorption of Cr (VI) and phenol onto tea waste biomass from binary mixture: multicomponent adsorption, thermodynamic and kinetic study. J Environ Chem Eng. 2015;3(2):785–96.

Jiang M, Han T, Wang J, Shao L, Qi C, Zhang XM, Liu C, Liu X. Removal of heavy metal chromium using cross-linked chitosan composite nanofiber mats. Int J Biol Macromol. 2018;120:213–21.

Karimi MA, Mohammadi SZ, Hatefi-Mehrjardi A, Mohadesi A, Yarahmadi J. A new sorbent based on MWCNTs modification for separation/preconcentration of trace amounts of Cd (II), Cr (III), Cu (II), Ni (II), and Pb (II) and their determination by flame atomic absorption spectrometry. J Anal Sci Technol. 2015;6(1):25.

Kaya M, Sargin I, Tozak KÖ, Baran T, Erdogan S, Sezen G. Chitin extraction and characterization from Daphnia magna resting eggs. Int J Biol Macromol. 2013;61:459–64.

Li S, Xu S, Liu S, Yang C, Lu Q. Fast pyrolysis of biomass in free-fall reactor for hydrogen-rich gas. Fuel Process Technol. 2004;85(8–10):1201–11.

Liu R, Zhang B, Mei D, Zhang H, Liu J. Adsorption of methyl violet from aqueous solution by halloysite nanotubes. Desalination. 2011;268(1–3):111–6.

Lussier MG, Shull JC, Miller DJ. Activated carbon from cherry stones. Carbon. 1994;32(8):1493–8.

Miretzky P, Cirelli AF. Hg (II) removal from water by chitosan and chitosan derivatives: a review. J Hazard Mater. 2009;167(1–3):10–23.

Mohan D, Pittman CU Jr. Activated carbons and low cost adsorbents for remediation of tri-and hexavalent chromium from water. J Hazard Mater. 2006;137(2):762–811.

Moon DH, Wazne M, Koutsospyros A, Christodoulatos C, Gevgilili H, Malik M, Kalyon DM. Evaluation of the treatment of chromite ore processing residue by ferrous sulfate and asphalt. J Hazard Mater. 2009;166(1):27–32.

Nyangababo J, Henry L, Omutange E. Heavy metal contamination in plants, sediments, and air precipitation of katonga, simiyu, and nyando wetlands of Lake Victoria basin, East Africa. Bull Environ Contam Toxicol. 2005;75(1):189–96.

Pandey S, Ramontja J. Guar gum-grafted poly (acrylonitrile)-templated silica xerogel: nanoengineered material for lead ion removal. J Anal Sci Technol. 2016;7(1):24.

Parlayıcı Ş. Modified peach stone shell powder for the removal of Cr (VI) from aqueous solution: synthesis, kinetic, thermodynamic, and modeling study. Int J Phytoremediation. 2019; (In press).

Parlayici S, Pehlivan E. Removal of metals by Fe3O4 loaded activated carbon prepared from plum stone (Prunus nigra): kinetics and modelling study. Powder Technol. 2017;317:23–30.

Rajput S, Pittman CU Jr, Mohan D. Magnetic magnetite (Fe3O4) nanoparticle synthesis and applications for lead (Pb2+) and chromium (Cr6+) removal from water. J Colloid Interface Sci. 2016;468:334–46.

Sargin İ, Arslan G. Effect of glutaraldehyde cross-linking degree of chitosan/
    sporopollenin microcapsules on removal of copper (II) from aqueous
    solution. Desalin Water Treat. 2015:1–13.

Sargın İ, Arslan G. Chitosan/sporopollenin microcapsules: preparation,
    characterisation and application in heavy metal removal. Int J Biol Macromol.
    2015;75(0):230–8.

Sari A, Tuzen M, Kocal İ. Application of chitosan-modified pumice for antimony
    adsorption from aqueous solution. Environ Prog Sustain Energy. 2017;36(6):
    1587–96.

Strelko V Jr, Malik D, Streat M. Characterisation of the surface of oxidised carbon
    adsorbents. Carbon. 2002;40(1):95–104.

Tahar LB, Oueslati MH, Abualreish MJA. Synthesis of magnetite derivatives
    nanoparticles and their application for the removal of chromium (VI) from
    aqueous solutions. J Colloid Interface Sci. 2018;512:115–26.

Tuzen M, Sarı A. Biosorption of selenium from aqueous solution by green algae
    (Cladophora hutchinsiae) biomass: equilibrium, thermodynamic and kinetic
    studies. Chem Eng J. 2010;158(2):200–6.

Wang J, Chen C. Biosorbents for heavy metals removal and their future.
    Biotechnol Adv. 2009;27(2):195–226.

Wu FC, Tseng RL, Juang RS. A review and experimental verification of using
    chitosan and its derivatives as adsorbents for selected heavy metals. J
    Environ Manag. 2010;91(4):798–806.

Wu Y, Ming Z, Yang S, Fan Y, Fang P, Sha H, Cha L. Adsorption of hexavalent
    chromium onto bamboo charcoal grafted by Cu2+-N-aminopropylsilane
    complexes: optimization, kinetic, and isotherm studies. J Ind Eng Chem.
    2017;46:222–33.

Wu Y, Wen Y, Zhou J, Cao J, Jin Y, Wu Y. Comparative and competitive
    adsorption of Cr (VI), As (III), and Ni (II) onto coconut charcoal. Environ Sci
    Pollut Res. 2013;20(4):2210–9.